



## Description and Performance of the COSINUS remoTES Design

V. Zema<sup>1</sup> · K. Shera<sup>1</sup> · G. Angloher<sup>1</sup> · M. R. Bharadwaj<sup>1</sup> · M. R. Cababie<sup>5,6</sup> ·  
I. Dafinei<sup>2,3</sup> · N. Di Marco<sup>2,4</sup> · L. Einfalt<sup>5,6</sup> · F. Ferroni<sup>2,3</sup> · S. Fichtinger<sup>5</sup> ·  
A. Filipponi<sup>4,7</sup> · T. Frank<sup>1</sup> · M. Friedl<sup>5</sup> · Z. Ge<sup>8</sup> · M. Heikinheimo<sup>9</sup> · M. N. Hughes<sup>1</sup> ·  
K. Huitu<sup>9</sup> · M. Kellermann<sup>1</sup> · R. Maji<sup>5,6</sup> · M. Mancuso<sup>1</sup> · L. Pagnanini<sup>2,4</sup> ·  
F. Petricca<sup>1</sup> · S. Pirro<sup>4</sup> · F. Pröbst<sup>1</sup> · G. Profeta<sup>4,7</sup> · A. Puiu<sup>4</sup> · F. Reindl<sup>5,6</sup> ·  
K. Schäffner<sup>1</sup> · J. Schieck<sup>5,6</sup> · D. Schmiedmayer<sup>5,6</sup> · P. R. Schreiner<sup>5,6</sup> ·  
C. Schwertner<sup>5,6</sup> · M. Stahlberg<sup>1</sup> · A. Stendahl<sup>9</sup> · M. Stukel<sup>2,4</sup> · C. Tresca<sup>4,10</sup> ·  
F. Wagner<sup>5</sup> · S. Yue<sup>8</sup> · Y. Zhu<sup>8</sup>

Received: 3 November 2023 / Accepted: 17 August 2024 / Published online: 31 August 2024

© The Author(s) 2024

### Abstract

COSINUS is a new cryogenic observatory for rare event searches located in the Laboratori Nazionali del Gran Sasso in Italy. COSINUS's first goal is to clarify whether the signal detected by the DAMA/LIBRA experiment originates from dark matter particle interactions or has a different nature. To this aim, sodium iodide (NaI) cryogenic scintillating calorimeters read out by transition edge sensors (TESs) are developed. To preserve the NaI crystal from the TES fabrication process, COSINUS implemented a novel design, the remoTES, where the TES is deposited on a separate wafer and coupled to the absorber through a Au-bonding wire and a Au-phonon collector. This design has reached baseline resolutions below 100 eV for Si, 200 eV for  $\text{TeO}_2$  and 400 eV for NaI absorbers. These results show that the remoTES not only brings COSINUS close to its performance goal of 1 keV energy threshold, but also offers the possibility to employ delicate crystals previously excluded for cryogenic applications as absorbers and to avoid the exposure of the absorbers to the TES fabrication process. It therefore extends the choice of target materials of the rare event searches using TES. In this work, we will provide a detailed description of the remoTES design and present the results of the latest prototypes.

**Keywords** TES · Rare-event-search · Calorimeters · Scintillation · NaI · Dark-matter

Extended author information available on the last page of the article

## 1 Introduction

Low-temperature detectors play a crucial role in the rare-event-searches for dark matter (DM) particles and neutrinos. One of the main advantages is the versatility of cryogenic calorimeters regarding the use of different absorber materials. Exemplary, in the field of DM direct detection, transition edge sensors (TESs) have been optimized to read out semiconductors like Si and Ge [1] and inorganic crystals scintillators like  $\text{CaWO}_4$ ,  $\text{ZnWO}_4$ ,  $\text{Al}_2\text{O}_3$ ,  $\text{LiMoO}_4$  or  $\text{LiAlO}_2$  [2]. However, materials which have a low melting point and are hygroscopic, like NaI, cannot withstand the standard TES fabrication processes. In the field of DM direct detection, NaI plays a special role as a target material since it is the crystal employed by the DAMA/LIBRA experiment. This latter operates NaI as a room temperature scintillator and claims the first observation of a DM signal [3, 4]. COSINUS (Cryogenic Observatory for Signals seen in Next generation Underground Searches) is a DM direct detection experiment employing NaI crystals as low-temperature calorimeters [5]. COSINUS engineered and successfully implemented a new coupling design of tungsten transition edge sensors (W-TESs) to the absorber, namely the remote TES (remoTES) [6]. By operating NaI as a cryogenic scintillating calorimeter read out with TESs, COSINUS is able to measure both the phonon and the light signal, thereby enabling particle identification on an event-by-event basis. This technique offers the possibility to unveil the nature of the annually modulating signal observed by DAMA/LIBRA. In this contribution, we describe the first tests of the remoTES coupling design on a NaI absorber [7, 8], as well as on Si and  $\text{TeO}_2$  [6]. Also, we present the ongoing studies for the optimization of the remoTES detectors [9].

## 2 The remoTES Design

The key mechanism of the cryogenic calorimeter working principle is the efficient collection of the phonons generated in the absorber by a particle interaction. The collection efficiency depends on the thermal coupling between the absorber and the sensor, which in turn depends on the acoustic matching between the sensor and the absorber material and the electron–phonon coupling in the sensor [10]. The W-TES serves both and is employed in many cryogenic experiments, e.g., [1, 2]. However, for the scientific goal of COSINUS, NaI is the required absorber crystal. Since NaI is hygroscopic and has a low melting point, it cannot survive the standard fabrication process of W-TES on its surface, which involves high temperatures for the deposition of the Al and W thin films as well as wet-chemistry during the lift-off-process. To overcome this, COSINUS implemented the remoTES, a novel TES-based design which was previously conceptually proposed in [11]. A schematic of the remoTES design is shown in Fig. 1 (left). The main difference with respect to previous calorimeter designs is the fabrication of the TES on a wafer separated from the absorber. The thermal coupling between TES

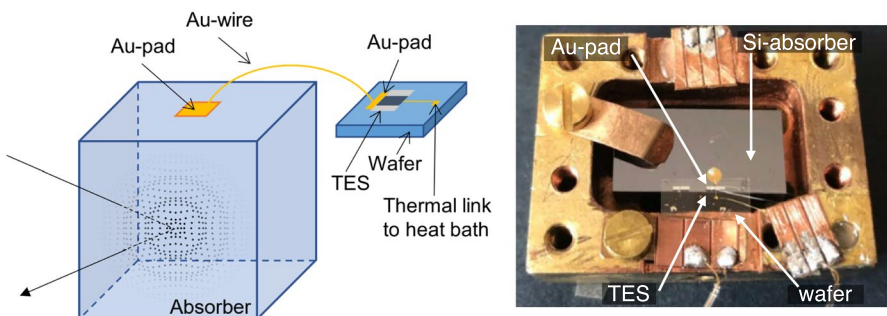


**Fig. 1** Left: A schematic representation of the remoTES design. Right: A picture of a Si-remoTES detector [6]

and absorber is obtained using a bonding wire and a phonon collector (Au-pad) placed on the absorber surface. Literature values of electron–phonon coupling in gold [10, 12] are similar or larger than the ones reported for tungsten [13]; thus, an efficient energy transfer from the phonon to the electron system in gold is expected. The Au-phonon-collector size, thickness and area can be tuned to increase the phonon collection efficiency while controlling the impact of the total heat capacity. To the same aim, different methods of fabrication of the Au-pad on the absorber surface (e.g., gluing, evaporation or sputtering) and the type of Au-pad (e.g., foils cut from Au-nuggets or films deposited directly on the absorber surface) can be tested. To restore the base temperature of the sensor, a Au-stripe thermally couples the TES to the heat bath by a bonding wire.

## 2.1 NaI-remoTEs

COSINUS has successfully applied the remoTES readout to NaI absorbers [7, 8]. We report here on the prototype with the best performance, which was achieved in an underground measurement performed at the CRESST test facility at LNGS [8]. A complete module with phonon and light detector was operated for an effective mass and time exposure of 11.6 g·days (gd). The absorber was a  $(10 \times 10 \times 10)$  cm $^3$  NaI, and the phonon collector was a 1  $\mu\text{m}$  thick foil of 1.8 mm $^2$  in area and glued with EPO-TEK 301-2. The Au-wire was a 17  $\mu\text{m}$  diameter wire, wedge-bonded on both sides. The W-TES was a  $(400 \times 100 \times 0.08)$   $\mu\text{m}^3$  film fabricated on a sapphire wafer of dimensions  $(10 \times 20 \times 0.5)$  mm $^3$ . The light detector was a beaker-shaped Si-crystal of 15 g (4 cm height, 4 cm outer diameter and 1 mm wall thickness) encapsulating the NaI-remoTES. The resolution achieved was  $(0.441 \pm 0.011)$  keV in the NaI-remoTES channel and  $(1.00 \pm 0.06)$  keVee (ee: electron-equivalent) in the light channel. With this measurement, particle discrimination on an event-by-event basis in NaI was demonstrated for the first time down to 4 keV by using an AmBe neutron source. Also, the light quenching factors for Na and I at around 15 mK were measured for the first time ( $QF_{Na}(10 \text{ keV}) = 0.20 \pm 0.01$  and  $QF_I(10 \text{ keV}) = 0.083 \pm 0.004$ ).

## 2.2 Si and $\alpha$ -TeO<sub>2</sub> remoTESs

The remoTES design has been applied also to Si and  $\alpha$ -TeO<sub>2</sub> absorbers [6]. The Si-remoTES was used to investigate the reach of the remoTES coupling design compared to other Si-based cryogenic calorimeters. Using a Si absorber of  $(20 \times 10 \times 5)$  mm<sup>3</sup>, equipped with a sputtered Au-film of 200 nm thickness with residual resistivity ratio (RRR)  $\simeq 3.8$ , a Au-wire of 17  $\mu\text{m}$  diameter glued with silver glue and a  $(220 \times 300 \times 0.1)$   $\mu\text{m}^3$  W-TES film evaporated on a Al<sub>2</sub>O<sub>3</sub> wafer of dimension  $(10 \times 10 \times 0.4)$  mm<sup>3</sup> (Fig. 1, right), a baseline resolution of  $(0.088 \pm 0.006)$  keV was achieved.

The  $\alpha$ -TeO<sub>2</sub> absorber features a similar phonon band structure as NaI, i.e., with a phonon band gap, and it is easy to handle since it is not hygroscopic. Thus, it is a suitable material for testing the remoTES concept for the application on NaI. After a series of measurements, the best performance was achieved using a  $(20 \times 10 \times 2)$  mm<sup>3</sup>  $\alpha$ -TeO<sub>2</sub>, with a Au-foil of 400 nm thickness (RRR  $\simeq 15$ ), glued with epoxy resin, two Au-wires of 17  $\mu\text{m}$  diameter wedge-bonded on both the TES and the absorber sides. The resulting baseline resolution was  $(0.194 \pm 0.004)$  keV [6].

## 3 Optimization Studies

The geometry and design of the remoTES components, along with the bonding technique used to connect the absorber to the TES can significantly influence the detector performance. To evaluate the impact of these components, systematic studies were conducted employing Si-crystals as a benchmark [9]. A detector consisted of a  $(20 \times 10 \times 5)$  mm<sup>3</sup> Si absorber, equipped with a Au-foil of 1  $\mu\text{m}$  thickness and 7.5 mm<sup>2</sup> area glued on the crystal surface using a two-component epoxy resin. The Au-foil and the TES were thermally connected using a 17- $\mu\text{m}$ -thick Au-wire, which was wedge-bonded on both sides. An  $^{55}\text{Fe}$  X-ray source with low count rate was mounted inside the module to calibrate the absorber events. Upon disassembling the detector, a thorough examination of the bond foot, conducted using a high-magnification microscope (see Fig. 2, left panel), revealed that the wedge-bond-foot tore the Au-foil. Consequently, the area available for phonon collection during the measurement was reduced.

An alternative to wedge-bonding is ball-bonding. This technique applies less bonding force, thus is less destructive for the foil and the absorber. This is particularly relevant for NaI, which is soft, and micro-fractures beneath the wedge-bond-foot were observed. Ball-bonding on 1  $\mu\text{m}$  glued Au-foil was unsuccessful. Inspecting the sample showed that the high temperature required to ball-bond melted and destroyed the glue between the thin Au-pad and the absorber. Instead, it was possible to ball-bond on Si-remoTES detectors with a 0.2  $\mu\text{m}$  thick sputtered Au-film and on a 8  $\mu\text{m}$  thick glued Au-foil. The area was in both cases equal to 3 mm<sup>2</sup>. On the TES side, the remoTESs were wedge-bonded. Additional  $^{55}\text{Fe}$  X-ray sources were placed to irradiate the Au-pads. The comparison of the baseline resolution of the detectors is reported in Table 1. By only considering heat capacities, a reduced performance

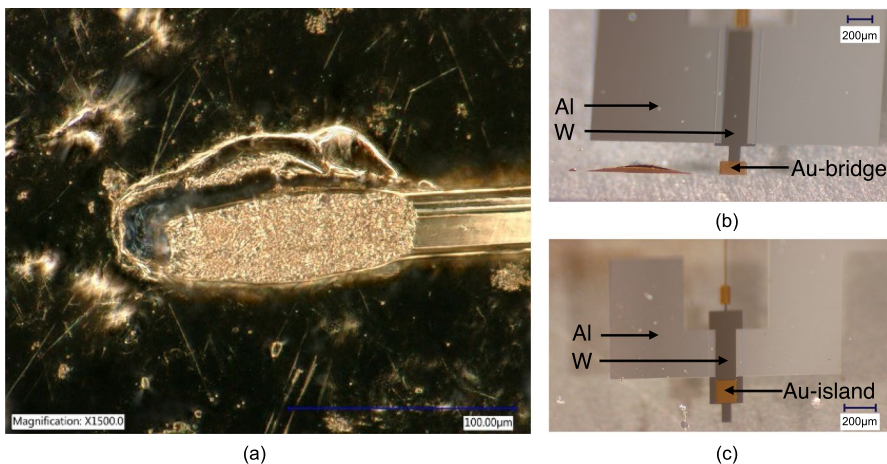


**Fig. 2** **a** Wedge-bond-foot detached from the 1  $\mu\text{m}$  glued Au-foil. The effect is the reduction of the Au-foil area available for phonon collection. **b** TES design with the Au-bridge. **c** TES design with the Au-island

**Table 1** Characteristics and performance of the Si-remoTES detectors.  $\sigma_{\text{res}}$  is their baseline resolution. The remoTES design is the Au-bridge for all the three measurements

Detector design and performance			
Au-pad size	Bonding	TES thickness (nm)	$\sigma_{\text{res}}$ (keV)
7.5 $\text{mm}^2 \times 1 \mu\text{m}$ (glued)	Wedge	156	$0.280 \pm 0.009$
3 $\text{mm}^2 \times 0.2 \mu\text{m}$ (sputtered)	Ball	450	$0.133 \pm 0.003$
3 $\text{mm}^2 \times 8 \mu\text{m}$ thick (glued)	Ball	460	$0.089 \pm 0.002$

for the detector with the thick glued Au-pad is expected. The comparison shows, instead, that this detector has the best baseline resolution. This observation further supports the hypothesis that the wedge-bond adversely affects the quality of the Au-foil and hinders signal transmission for thin glued Au-foils. Furthermore, when comparing the two ball-bonded Si-remoTES detectors, it was observed that the performance of the detector with the thicker Au-foil was superior. This suggests that the heat capacity is not (yet) the limiting factor. A hypothesis is that in Si-remoTESs the presence of the glue has a positive impact on the signal collection. Further systematic studies to verify these hypotheses are required. The pulse shapes of the Au-pad events of the two Si-remoTESs with the ball-bond are shown in Fig. 3 (left). The comparison shows that the detector with larger heat capacity (thicker Au-pad) shows a larger thermal component (tail of the pulse).

The TES design of the 8  $\mu\text{m}$  thick glued Au-foil detector featured a Au-bonding-pad that partially overlapped with the W-film, labeled “Au-bridge” in the following (see Fig. 2b). To test the thermal conductance of the Au-bridge, this latter was modified and the Au-bonding-pad was deposited entirely on the W-film and labeled

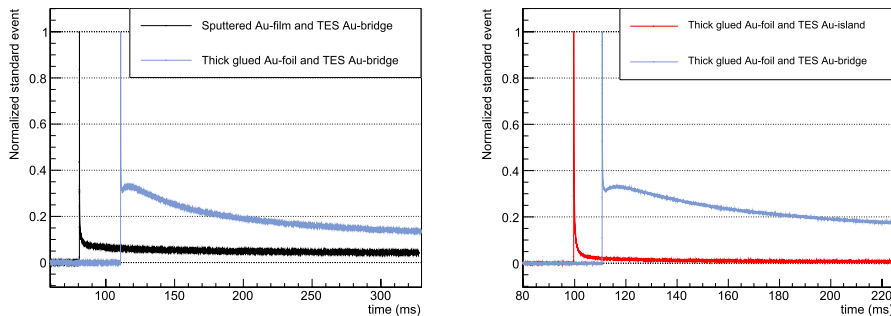


**Fig. 3** Left: Pulse shape of the Au-events in the thick glued Au-foil (light blue) and sputtered Au-film (black). Right: Pulse shape of Au-events in the thick glued Au-foil connected to a Au-bridge TES (light blue) and in the thick glued Au-foil connected to a Au-island TES (red) (Color figure online)

“Au-island” (see Fig. 2c). The impact of this modification was assessed by studying the events produced by the direct hits of an  $^{55}\text{Fe}$  source on the Au-phonon collectors. The distinct pulse shapes of these events are shown in Fig. 3, right panel. While the remoTES with the Au-bridge (depicted in light blue) features a very sharp rise but a slow decaying tail that does not decay within the record window, the pulse shape of the events in the Au-island remoTES (depicted in red) does not show the slow decaying tail and exhibits a much faster decay. A plausible explanation for the slow decaying tail is a poor signal conductance to the TES. The presence of the Au-bridge is a bottleneck in the Au/W-interface, impeding signal transmission and causing a backflow of the signal to the Au-pad. Additionally, the partial thermal contact of the Au-bridge with the sapphire wafer can be considered as a signal-loss channel. According to these results, the default remoTES design was modified by replacing the Au-bridge with the Au-island. In addition to refine the gluing technique, COSINUS is investigating the performance of evaporated Au-films (shadow mask) on NaI, which were successfully fabricated thanks to the collaboration of R. Götz and A. Bandarenka (Technical University of Munich (TUM), School of Natural Sciences, Department of Physics, Physics of Energy Conversion and Storage).

## 4 Conclusions

The remoTES design offers the possibility of using delicate target materials like NaI as cryogenic calorimeters, while at the same time simplifying the detector scalability. Its implementation was successful and resulted into a baseline resolution of  $(0.441 \pm 0.011)$  keV,  $(0.194 \pm 0.004)$  keV and  $(0.088 \pm 0.006)$  keV in NaI-,  $\text{TeO}_2$ - and Si-remoTESs, respectively. Systematic studies carried out on Si-remoTESs showed that (i) ball-bonding on thick glued Au-foils (8  $\mu\text{m}$ ) improves

the thermal conductance and (ii) the Au-island remoTES design improves the performance. According to these results, the COSINUS experiment plans to employ remoTES wafers with the Au-island design, ball-bonded to the Au-pad. The optimization of the thermal coupling of the Au-pad to the NaI absorber is ongoing,

with the first evaporation process of Au-films on NaI being successful. The finalization of the COSINUS detector design is anticipated by 2024. An answer to what is the nature of the signal detected by DAMA/LIBRA is expected by 2027.

**Acknowledgements** We are very grateful to the CRESST group at the Max Planck Institute for Physics (MPP) for sharing the use of the cryogenic facilities that made this work possible, the mechanical workshop of MPP for the invaluable support and SICCAS for producing the NaI crystal employed in the measurement described in this work. This work has been supported by the Austrian Science Fund FWF, stand-alone project AnaCONDA [P 33026-N]. This project was supported by the Austrian Research Promotion Agency (FFG), project ML4CPD.

**Author contributions** VZ and Kumrie Shera (KS) wrote the manuscript. The work reported in the “Optimization studies” section was performed during KS’s Master thesis. All authors reviewed the manuscript.

**Funding** Open Access funding enabled and organized by Projekt DEAL.

## Declarations

**Competing interests** The authors declare no competing interests.

**Open Access** This article is licensed under a Creative Commons Attribution 4.0 International License, which permits use, sharing, adaptation, distribution and reproduction in any medium or format, as long as you give appropriate credit to the original author(s) and the source, provide a link to the Creative Commons licence, and indicate if changes were made. The images or other third party material in this article are included in the article’s Creative Commons licence, unless indicated otherwise in a credit line to the material. If material is not included in the article’s Creative Commons licence and your intended use is not permitted by statutory regulation or exceeds the permitted use, you will need to obtain permission directly from the copyright holder. To view a copy of this licence, visit <http://creativecommons.org/licenses/by/4.0/>.

## References

1. I. Alkhateeb, et al., Light dark matter search with a high-resolution athermal phonon detector operated above ground. *Phys. Rev. Lett.* **127**(6), 061801 (2021). <https://doi.org/10.1103/PhysRevLett.127.061801>
2. G. Angloher, et al., Results on sub-GeV dark matter from a 10 eV threshold CRESST-III silicon detector. *Phys. Rev. D* **107**(12), 122003 (2023). <https://doi.org/10.1103/PhysRevD.107.122003>. [arXiv:2212.12513](https://arxiv.org/abs/2212.12513)
3. R. Bernabei, et al., Recent results from DAMA/LIBRA and comparisons. *Mosc. Univ. Phys. Bull.* **77**(2), 291–300 (2022). <https://doi.org/10.15407/jnpae2021.04.329>
4. R. Bernabei, et al., Dark Matter with DAMA/LIBRA and its perspectives. *J. Phys.: Conf. Ser.*, 2586012096 (2023). <https://doi.org/10.1088/1742-6596/2586/1/012096>
5. K. Schäffner, et al., A NaI-based cryogenic scintillating calorimeter: results from a COSINUS prototype detector. *J. Low Temp. Phys.* **193**(5–6), 1174–1181 (2018). <https://doi.org/10.1007/s10909-018-1967-3>
6. G. Angloher et al., First measurements of remoTES cryogenic calorimeters: easy-to-fabricate particle detectors for a wide choice of target materials. *Nucl. Instrum. Meth. A* **1045**, 167532 (2023) <https://doi.org/10.1016/j.nima.2022.167532>. [arXiv:2111.00349](https://arxiv.org/abs/2111.00349) [physics.ins-det]
7. G. Angloher, et al., Particle discrimination in a NaI crystal using the COSINUS remote TES design (2023). [arXiv:2307.11066](https://arxiv.org/abs/2307.11066) [physics.ins-det]
8. G. Angloher, et al., Deep-underground dark matter search with a COSINUS detector prototype (2023) [arXiv:2307.11139](https://arxiv.org/abs/2307.11139) [astro-ph.CO]
9. K. Shera, Studies on remoTES-based Cryogenic Calorimeters for the COSINUS Experiment. Master’s thesis, Technical University of Munich and Max Planck Institute for Physics (2023)
10. F. Pröbst, et al., Model for cryogenic particle detectors with superconducting phase transition thermometers. *J. Low Temp. Phys.* **100**, 69–104 (1995). <https://doi.org/10.1007/BF00753837>

11. M. Pyle, et al., Optimized Designs for Very Low Temperature Massive Calorimeters (2015) [arXiv: 1503.01200](https://arxiv.org/abs/1503.01200) [astro-ph.IM]
12. J. Karvonen, et al., Electron–phonon interaction in thin copper and gold films. *Physica Status Solidi (c)* **1**(11), 2799–2802 (2004). <https://doi.org/10.1002/pssc.200405326>
13. M. Sisti, et al., Massive cryogenic particle detectors with low energy threshold. *Nucl. Instrum. Meth. A* **466**(3), 499–508 (2001). [https://doi.org/10.1016/S0168-9002\(01\)00801-4](https://doi.org/10.1016/S0168-9002(01)00801-4)

## Authors and Affiliations

**V. Zema**<sup>1</sup> · **K. Shera**<sup>1</sup> · **G. Angloher**<sup>1</sup> · **M. R. Bharadwaj**<sup>1</sup> · **M. R. Cababie**<sup>5,6</sup> ·  
**I. Dafinei**<sup>2,3</sup> · **N. Di Marco**<sup>2,4</sup> · **L. Einfalt**<sup>5,6</sup> · **F. Ferroni**<sup>2,3</sup> · **S. Fichtinger**<sup>5</sup> ·  
**A. Filipponi**<sup>4,7</sup> · **T. Frank**<sup>1</sup> · **M. Friedl**<sup>5</sup> · **Z. Ge**<sup>8</sup> · **M. Heikinheimo**<sup>9</sup> · **M. N. Hughes**<sup>1</sup> ·  
**K. Huitu**<sup>9</sup> · **M. Kellermann**<sup>1</sup> · **R. Maji**<sup>5,6</sup> · **M. Mancuso**<sup>1</sup> · **L. Pagnanini**<sup>2,4</sup> ·  
**F. Petricca**<sup>1</sup> · **S. Pirro**<sup>4</sup> · **F. Pröbst**<sup>1</sup> · **G. Profeta**<sup>4,7</sup> · **A. Puiu**<sup>4</sup> · **F. Reindl**<sup>5,6</sup> ·  
**K. Schäffner**<sup>1</sup> · **J. Schieck**<sup>5,6</sup> · **D. Schmiedmayer**<sup>5,6</sup> · **P. R. Schreiner**<sup>5,6</sup> ·  
**C. Schwertner**<sup>5,6</sup> · **M. Stahlberg**<sup>1</sup> · **A. Stendahl**<sup>9</sup> · **M. Stukel**<sup>2,4</sup> · **C. Tresca**<sup>4,10</sup> ·  
**F. Wagner**<sup>5</sup> · **S. Yue**<sup>8</sup> · **Y. Zhu**<sup>8</sup>

✉ V. Zema  
vanessa.zema@mpp.mpg.de

✉ K. Shera  
kshera@mpp.mpg.de

<sup>1</sup> Max-Planck-Institut für Physik, 80805 München, Germany

<sup>2</sup> Gran Sasso Science Institute, 67100 L’Aquila, Italy

<sup>3</sup> INFN - Sezione di Roma, 00185 Rome, Italy

<sup>4</sup> INFN - Laboratori Nazionali del Gran Sasso, 67100 Assergi, Italy

<sup>5</sup> Institut für Hochenergiephysik der Österreichischen Akademie der Wissenschaften, 1050 Wien, Austria

<sup>6</sup> Atominstitut, Technische Universität Wien, 1020 Wien, Austria

<sup>7</sup> Dipartimento di Scienze Fisiche e Chimiche, Università degli Studi dell’Aquila, 67100 L’Aquila, Italy

<sup>8</sup> SICCAS - Shanghai Institute of Ceramics, Shanghai 200050, People’s Republic of China

<sup>9</sup> Helsinki Institute of Physics, University of Helsinki, 00014 Helsinki, Finland

<sup>10</sup> CNR-SPIN c/o Dipartimento di Scienze Fisiche e Chimiche, Università degli studi dell’Aquila, 67100 L’Aquila, Italy